Low-cost functional plasticity of TRPV1 supports heat tolerance in squirrels and camels

Willem J. Laursen[a,b,c], Eve R. Schneider[a], Dana K. Merriman[d], Sviatoslav N. Bagriantsev[a,1], and Elena O. Gracheva[a,b,c,1]

[a]Department of Cellular & Molecular Physiology, Yale University School of Medicine, New Haven, CT 06510; [b]Department of Neuroscience, Yale University School of Medicine, New Haven, CT 06510; [c]Program in Cellular Neuroscience, Neurodegeneration and Repair, Yale University School of Medicine, New Haven, CT 06510; and [d]Department of Biology, University of Wisconsin, Oshkosh, WI 54901

Edited by Joseph S. Takahashi, Howard Hughes Medical Institute, University of Texas Southwestern Medical Center, Dallas, TX, and approved July 26, 2016 (received for review March 14, 2016)

The ability to sense heat is crucial for survival. Increased heat tolerance may prove beneficial by conferring the ability to inhabit otherwise prohibitive ecological niches. This phenomenon is widespread and is found in both large and small animals. For example, ground squirrels and camels can tolerate temperatures more than 40 °C better than many other mammalian species, yet a molecular mechanism subserving this ability is unclear. Transient receptor potential vanilloid 1 (TRPV1) is a polymodal ion channel involved in the detection of noxious thermal and chemical stimuli by primary afferents of the somatosensory system. Here, we show that thirteen-lined ground squirrels (*Ictidomys tridecemlineatus*) and Bactrian camels (*Camelus ferus*) express TRPV1 orthologs with dramatically reduced temperature sensitivity. The loss of sensitivity is restricted to temperature and does not affect capsaicin or acid responses, thereby maintaining a role for TRPV1 as a detector of noxious chemical cues. We show that heat sensitivity can be reengineered in both TRPV1 orthologs by a single amino acid substitution in the N-terminal ankyrin-repeat domain. Conversely, reciprocal mutations suppress heat sensitivity of rat TRPV1, supporting functional conservation of the residues. Our studies suggest that squirrels and camels co-opt a common molecular strategy to adapt to hot environments by suppressing the efficiency of TRPV1-mediated heat detection at the level of somatosensory neurons. Such adaptation is possible because of the remarkable functional flexibility of the TRPV1 molecule, which can undergo profound tuning at the minimal cost of a single amino acid change.

TRPV1 | thermosensation | thirteen-lined ground squirrel | bactrian camel | sensory physiology

The somatosensory system allows animals to distinguish between innocuous and noxious temperatures, guiding them to environments most amenable for life and reproduction. In general, mammals avoid contacting surfaces heated more than 40 °C, which helps stave off the danger of tissue damage, but at the same time limits inhabitable areas. Mammalian extremophiles such as camels and diurnal rodents, including ground squirrels and chipmunks (Fig. 1*A*), thrive under thermal conditions that are harmful or even fatal to other animals. The mechanism(s) that allows such species to cope with high temperatures are complex and involve various organs and tissues, including thermoregulatory and somatosensory systems (1–5), but the exact molecular adaptations remain enigmatic.

In rodents, noxious stimuli, including temperature, are detected in the skin by the terminal endings of C-type nociceptors from dorsal root or trigeminal ganglia marked by the expression of the heat-activated ion channel transient receptor potential vanilloid 1 (TRPV1) (6–9). Deletion of *Trpv1* in mice does not abolish pain sensitivity in general (10) but diminishes sensitivity to noxious temperatures more than 50 °C (7, 8). Whereas the general pathways of heat sensitivity in standard laboratory rodents has been worked out in some detail, little is known about molecular adaptations in other animals, especially in the mammalian heat extremophiles. Indeed, it remains unclear whether the TRPV1-centered molecular mechanism of heat sensitivity in mice and rats represents a conserved evolutionary strategy adopted by many species (11, 12). Such questions are best elucidated by using animals that took heat sensitivity to the extreme. Here, we explored the molecular basis of heat tolerance at the level of somatosensory system by using two evolutionarily distant species of extremophiles: thirteen-lined ground squirrel (*Ictidomys tridecemlineatus*) and wild Bactrian camel (*Camelus ferus*).

Results

TRPV1$^+$ Nociceptors from Ground Squirrels Are Poorly Sensitive to Temperature. We compared temperature preference in mice and squirrels by using the standard two-plate temperature preference test, whereby an animal is given a choice to stay on a reference plate set to 25 °C or move to a test plate with variable temperature. Consistent with earlier data (13), mice preferred the 25 °C plate when the test plate was set to 45 °C or above. In contrast, squirrels began to show preference for the reference plate only when the temperature of the test plate reached 55 °C (Fig. 1*B*). The difference in behavior between mice and squirrels is striking and cannot be explained simply by the animals' size, because earlier studies showed that rats, which are bigger than squirrels, avoid heat similar to mice in the same experimental conditions (14). The apparent heat tolerance observed in squirrels could be explained by a number of scenarios, including a

Significance

Thirteen-lined ground squirrels and Bactrian camels are capable of withstanding elevated environmental temperatures. In mammals, the polymodal transient receptor potential vanilloid 1 (TRPV1) ion channel responds to temperatures >40 °C and marks peripheral neurons responsible for detecting noxious heat. However, we find that both squirrels and camels express TRPV1 channels with dramatic decreases in thermosensitivity in the physiologically relevant range. To regain heat sensitivity, squirrel and camel TRPV1 require substitution of a single conserved amino acid. These data point to a common molecular mechanism used by camels and squirrels to adapt to high temperatures and reveal a remarkable functional plasticity of temperature activation of the TRPV1 channel.

Author contributions: W.J.L., E.R.S., S.N.B., and E.O.G. designed research; W.J.L., E.R.S., S.N.B., and E.O.G. performed research; D.K.M. contributed new reagents/analytic tools; W.J.L., S.N.B., and E.O.G. analyzed data; W.J.L., E.R.S., S.N.B., and E.O.G. wrote the paper; D.K.M. supplied squirrels and advised on behavioral experiments; and S.N.B. and E.O.G. conceived the study and provided guidance and supervision throughout the project.

The authors declare no conflict of interest.

This article is a PNAS Direct Submission.

Data deposition: The sequence reported in this paper has been deposited in the GenBank database (accession no. KU877439).

[1]To whom correspondence may be addressed. Email: elena.gracheva@yale.edu or slav.bagriantsev@yale.edu.

This article contains supporting information online at www.pnas.org/lookup/suppl/doi:10.1073/pnas.1604269113/-/DCSupplemental.

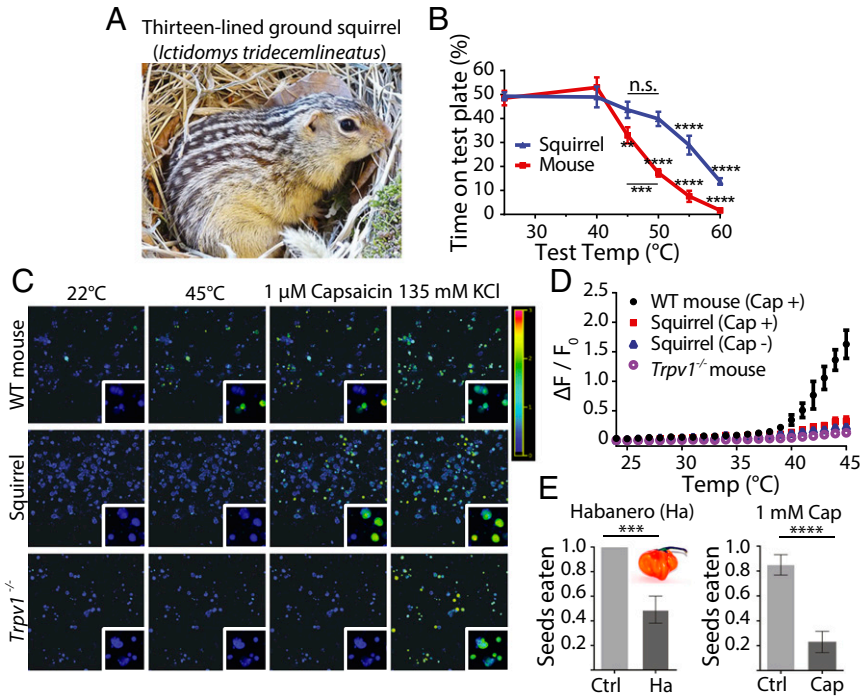

Fig. 1. Heat responses of primary afferent neurons are suppressed in thirteen-lined ground squirrels. (*A*) Image of a thirteen-lined ground squirrel. (*B*) Quantification of animal behavior in a temperature preference test shows the percentage of time spent on the control (25 °C) vs. test (25–60 °C) plate over 5 min. Data collected from ≥12 mice and ≥18 squirrels for each temperature point. $^{**}P < 0.01$, $^{***}P < 0.001$, $^{****}P < 0.0001$, one-way ANOVA with Dunnett post hoc test vs. 25 °C, or Student's *t* test (45 °C vs. 50 °C). (*C* and *D*) Exemplar images (*C*) and quantification (*D*) of responses of dissociated DRG neurons to temperature and indicated chemicals obtained by ratiometric calcium imaging. Color coding in *C* denotes lowest and highest cytoplasmic calcium concentrations from bottom to top. Data was obtained from 78 wild-type and 788 *Trpv1*$^{-/-}$ mouse neurons, 714 capsaicin-sensitive, and 575 capsaicin-insensitive squirrel neurons. (*E*) Quantification of the amount of habanero pepper extract- or capsaicin-treated sunflower seeds consumed by same squirrel in 10 min. Data shown as mean ± SEM from ≥10 squirrels. $^{***}P < 0.001$, $^{****}P < 0.0001$, n.s., not significant, Student's paired *t* test.

diminished ability to detect high temperature at the level of peripheral afferents.

In mammals, noxious heat is detected by somatosensory neurons expressing TRPV1, a polymodal ion channel activated by hot temperatures, acidic pH, and capsaicin, the pungent agent from spicy peppers (6–8, 13, 15–18). TRPV1 is a marker of nociceptors and thermoreceptors and is expressed in 40–60% of mouse neurons from trigeminal or dorsal root ganglia (DRG) (19–21). Using RNA in situ hybridization, we estimated that 56.3 ± 1.2% of squirrel DRG neurons express TRPV1 (Fig. S1), indicating their apparent heat tolerance cannot be explained by a paucity of TRPV1-expressing neurons. To assess the functional properties of primary afferents, we analyzed the heat and capsaicin sensitivity of dissociated mouse and squirrel DRG neurons by live-cell ratiometric calcium imaging (Fig. 1*C* and Fig. S2). As expected, mouse neurons sensitive to 1 μM capsaicin were also activated at 40 °C. In contrast, although 57.2 ± 4.6% of squirrel neurons responded to 1 μM capsaicin, they failed to respond to a temperature ramp from 22 °C to 45 °C. The temperature-activation profiles of squirrel capsaicin-sensitive and capsaicin-insensitive neurons were indistinguishable from each other and from mouse *Trpv1*$^{-/-}$ cells (Fig. 1 *C* and *D* and Fig. S2), suggesting that squirrel neurons express TRPV1 with normal capsaicin- but ablated temperature-sensing properties. In agreement with the neuronal sensitivity to capsaicin, squirrels exhibited a significantly suppressed consumption rate of sunflower seeds infused with either habanero pepper extract or 1 mM capsaicin (Fig. 1*E*), demonstrating that the TRPV1 nociceptive pathway is intact. Together, our results support the notion that the apparent temperature-resistant phenotype of the squirrels could be subserved, at least in part, by the diminished temperature sensitivity of TRPV1-expressing neuronal thermoreceptors.

SqTRPV1 and CaTRPV1 Are Ion Channels with Diminished Heat Sensitivity. To test whether TRPV1 directly contributes to the neuronal phenotype, we cloned the channel from squirrel DRG and analyzed its biophysical properties by two-electrode voltage clamp in *Xenopus* oocytes. SqTRPV1 is 90% identical to the rat ortholog at the amino acid level (Fig. S3). We found that, although sqTRPV1, mTRPV1, and rTRPV1 have similar sensitivities to capsaicin (EC_{50}, mean ± SEM: 528.5 ± 32 nM, 775.6 ± 52 nM, and 527.1 ± 53 nM for sqTRPV1, mTRPV1, and rTRPV1, respectively, $n \geq 10$), sqTRPV1 failed to activate in response to a 22–46 °C temperature ramp, whereas mTRPV1 and rTRPV1 produced robust current with an apparent activation threshold at approximately 40 °C (Fig. 2 *A*–*C*, E, and F and Fig. S4). The heat-activated two-pore potassium channel TREK1 ($K_{2P}2.1$) is expressed in TRPV1 neurons, where it was proposed to function as a negative regulator of the heat-evoked excitability triggered by TRPV1 through a concurrent efflux of potassium (22, 23). We found that mouse and squirrel TREK1 channels have indistinguishable heat-activation properties in oocytes, suggesting that decreased temperature sensitivity is not a generalizable feature of the heat-activated ion channels found in the squirrel somatosensory system (Fig. 2 *G*–*I*). We further tested heat sensitivity of sqTRPV1 and rTRPV1 in human embryonic kidney 293T (HEK293T) cells. Similar to oocytes, both channels produced robust activity in response to 1 μM capsaicin, although the current appears to be less rectifying. In addition, rTRPV1 was activated by heat, whereas sqTRPV1 exhibited activity similar to control cells (Fig. 3). These results demonstrate that the suppressed heat sensitivity of sqTRPV1 does not depend on the cellular context. Given the correlation between heat responses of DRG neurons and TRPV1, we examined properties of sqTRPV1 further.

In the rat channel, heat sensitivity is known to be potentiated by protons: rTRPV1 exhibits similar basal activity at pH 7.4 and pH 6.3 at room temperature, but the acidic pH potentiates the channel's heat responses, leading to a leftward shift in the apparent temperature threshold by 3.6 °C (T_{act}, mean ± SEM: 40.1 ± 1.1 °C at pH 7.4; 36.5 ± 1.6 °C at pH 6.3, $n \geq 6$; Fig. 4 *A* and *B* and Fig. S5) (15). We found that sqTRPV1 has a slightly rightward shifted pH sensitivity ($pH_{1/2}$, mean ± SEM: 5.13 ± 0.02 and 5.49 ± 0.01 for rTRPV1 and sqTRPV1, respectively, $n \geq 10$), but similar to rTRPV1, remains inactive at pH 6.3. Despite the slightly higher overall sensitivity to protons of sqTRPV1, pH 6.3 failed to significantly potentiate heat responses of the channel (Fig. 4*B* and Fig. S5), suggesting that sqTRPV1 is insensitive to

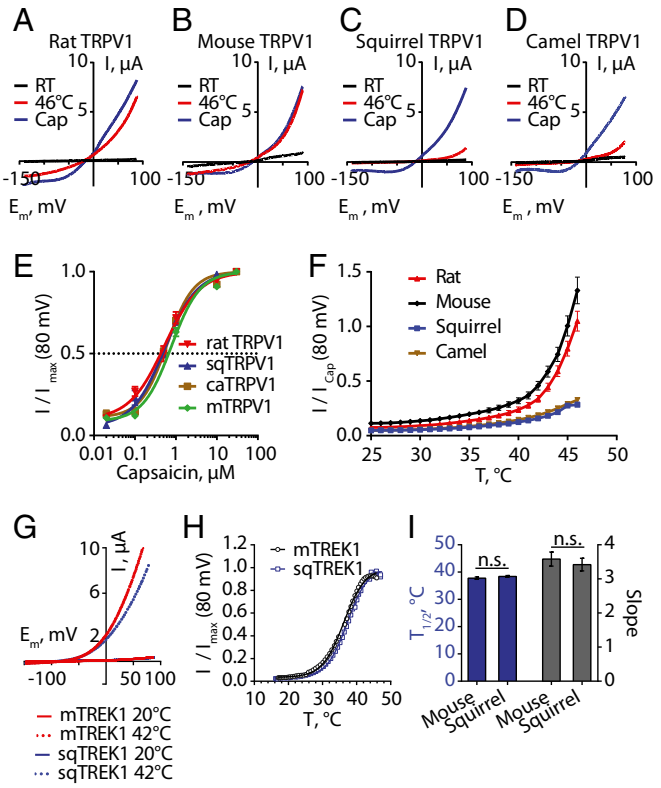

Fig. 2. SqTRPV1 and caTRPV1 are resistant to heat activation. Exemplar current–voltage plots of responses to capsaicin or temperature (46 °C) obtained by two-electrode voltage clamp in *Xenopus* oocytes expressing rTRPV1 (*A*), mTRPV1 (*B*), sqTRPV1 (*C*) and caTRPV1 (*D*). Currents were elicited by a voltage ramp from a holding potential of –80 mV. (*E*) Capsaicin dose–response curves for the indicated TRPV1 orthologs ($n \geq 10$). (*F*) Heat–response profiles for TRPV1 orthologs normalized to the maximum response of each oocyte to 5 μM capsaicin ($n \geq 18$). Exemplar current–voltage plot (*G*), heat response profile (*H*), and quantification of $T_{1/2}$ and slope for mouse and squirrel orthologs of TREK1 ($K_{2P}2.1$) (*I*), expressed in *Xenopus* oocytes. Data shown as mean ± SEM, $n \geq 11$. n.s., not significant, *t* test.

heat within the experimentally testable temperature range, and that the poor temperature sensitivity of sqTRPV1 does not result from altered pH sensitivity. Temperature sensitivity of the related TRPV2 channel has been shown to be use-dependent such that repetitive application of heat leads to significantly increased activity (24). However, consecutive heat ramps only minimally potentiated responses in rTRPV1 (1.7 ± 0.1 fold at +80 mV) and had no effect on sqTRPV1 (Fig. 4 *C* and *E*). However, the application of heat in the presence of a subthreshold concentration of capsaicin (100 nM) potentiated heat response from rTRPV1 (3.4 ± 0.4 and 5.8 ± 1.2 fold at +80 mV and −80 mV, respectively) and sqTRPV1 (2.7 ± 0.2 and 2.7 ± 0.5 fold at +80 mV and −80 mV, Fig. 4 *D* and *E*). These data suggest that sqTRPV1 is, in principle, sensitive to heat, but its apparent temperature activation threshold is shifted beyond testable or physiologically relevant range, unless the channel is sensitized with chemical agonist. Together, these data demonstrate that sqTRPV1 properties explain the temperature and capsaicin sensitivity of somatosensory neurons and provide a molecular basis for the apparent heat resistance in the behavioral test.

We next sought to examine functional properties of TRPV1 from a phylogenetically distant temperature extremophile, the wild Bactrian camel (*Camelus ferus*). The predicted camel TRPV1 is 85% and 89% identical to the rat and squirrel orthologs, respectively (Fig. S3). We found that, similar to the squirrel channel, camel TRPV1 fails to respond to a 22–46 °C temperature ramp, although it retains normal capsaicin responses (EC_{50}, mean ± SEM: 609.6 ± 36 nM, $n = 10$) (Fig. 2 D–F). Our data reveal a remarkable correlation between the ability of squirrels and camels to cope with high environmental temperatures and diminished heat sensitivity of the TRPV1 channel.

A Single Conserved Amino Acid Substitution Restores Heat Sensitivity in SqTRPV1 and CaTRPV1. Because, to our knowledge, all other tested vertebrate TRPV1 orthologs exhibit robust heat activation in the 28–46 °C range (11, 12, 25), we attempted to reverse-engineer heat sensitivity in the squirrel and camel channels. The substitution of the whole cytosolic N terminus of sqTRPV1 (amino acids 1–430) with the same region from rTRPV1 (amino acids 1–428) resulted in heat-activated chimeras indistinguishable from the rat channel (Fig. S6). By systematically replacing N-terminal regions in squirrel and camel TRPV1, we narrowed the area of interest to a single pair of amino acids: Asn126/Glu190 and Asn124/Glu188, in squirrel and camel channels, respectively (Fig. 5 *A* and *B*). Single or double substitutions of these amino acids with the homologous residues from rTRPV1 (Ser124/Gln188, respectively) resulted in heat-activated sqTRPV1 mutants (Fig. 5 *C* and *D* and Fig. S6 *E–G*) without altering capsaicin sensitivity (Fig. S7 and Table S1). A similar gain of heat sensitivity was achieved in camel TRPV1 mutants (Fig. 5*E* and *F* and Fig. S6 *J–L*). Of the six tested single and double mutants, $sqTRPV1^{E190Q}$ showed only a mild heat response, whereas the rest were either indistinguishable from rTRPV1 ($sqTRPV1^{N126S/E190Q}$, $sqTRPV1^{N126S}$, $caTRPV1^{N124S/E188Q}$) or exhibited even more robust heat activation ($caTRPV1^{N124S}$, $caTRPV1^{E188Q}$), as judged by the normalized current amplitude at 44 °C (Fig. 5 *C–F* and Fig. S6 *E–G* and *J–L*). Thus, sqTRPV1 and caTRPV1 can acquire heat sensitivity comparable to that of the rat channel via a single conserved amino acid substitution. Conversely, reciprocal point mutations in

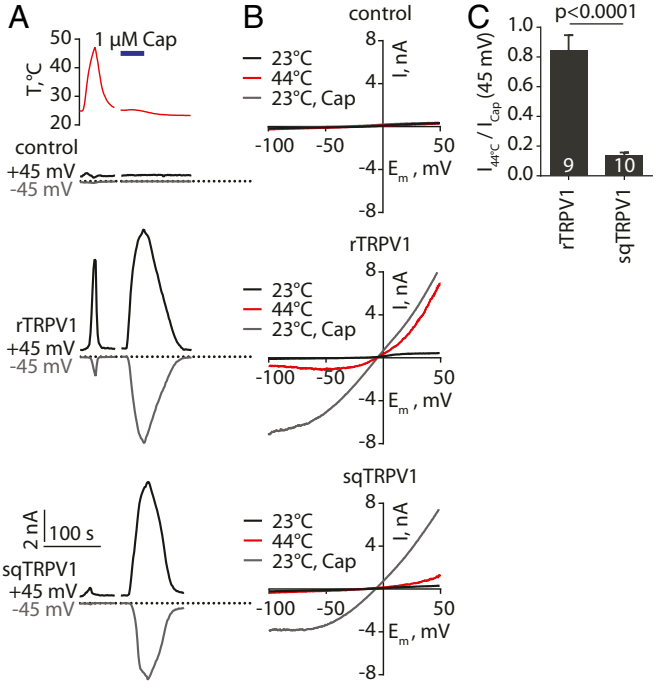

Fig. 3. Temperature responses of rTRPV1 and sqTRPV1 in HEK293T cells. Exemplar traces (*A*) and current–voltage plots (*B*) from whole-cell voltage-clamp recordings of HEK293T cells transiently transfected with eGFP (control), rTRPV1, and sqTRPV1). (*C*) Quantification of TRPV1 activity at 44 °C normalized to maximal activity evoked by 1 μM capsaicin ($n \geq 9$). Data shown as mean ± SEM, $P < 0.0001$, unpaired *t* test.

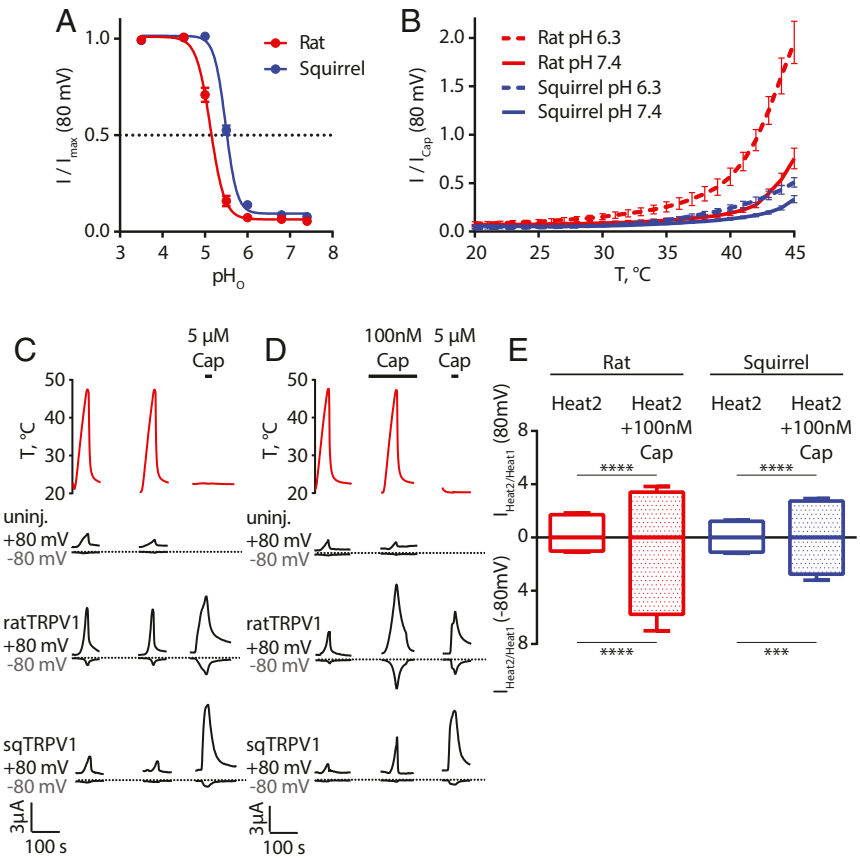

Fig. 4. Chemical and use-dependent modulation of TRPV1 thermosenstivity. (*A*) Proton concentration–response curves for TRPV1 orthologs in oocytes. Data shown as mean ± SEM ($n \geq 10$) and fitted to a modified Hill equation. (*B*) Effect of pH on temperature activation as shown by heat responses of rTRPV1 and sqTRPV1 at pH 7.4 and 6.3. Recordings were normalized to maximum responses of each oocyte to 5 µM capsaicin ($n \geq 6$). (*C* and *D*) Voltage-clamp recordings from oocytes in response to consecutive heat ramps. The second heat ramp was recorded in either standard physiological Ringer's solution (*C*) or with the addition of 100 nM capsaicin (*D*). (*E*) Quantification of maximum current at +80mV and −80mV evoked by the second heat application (with or without 100 nM capsaicin) relative to the maximal response in the first heat ramp. Data shown as mean ± SEM from 7 to 18 oocytes. ***$P < 0.001$, ****$P < 0.0001$, unpaired *t* test.

rat TRPV1 (rTRPV1^{S124N}, rTRPV1^{Q188E}, rTRPV1$^{S124N/Q188E}$) substantially reduced heat responses of the channel, suggesting functional conservation of the amino acids among the TRPV1 orthologs (Fig. 5 *G* and *H*).

Discussion

Our data show that two phylogenetically distant species of animals—ground squirrels and camels—known for their ability to withstand high environmental temperatures, possess TRPV1 orthologs with poor heat-activating properties. In heterologous systems, sqTRPV1 and caTRPV1 fail to exhibit significant temperature activation in the experimentally testable range of up to 46 °C. Temperatures above this limit evoke robust background current in naïve *Xenopus* oocytes and HEK293T cells, preventing us from accurately assessing channel properties at higher temperatures. Therefore, although we do not rule out the possibility that sqTRPV1 and caTRPV1 may exhibit activation at temperatures higher than 46 °C, they are the poorest heat sensors of all known vertebrate TRPV1 orthologs in the experimentally testable range (11, 12, 25).

The striking correlation between the behavior of the animals and properties of the channel support the idea that TRPV1 is a key somatosensory receptor of noxious heat. Our temperature preference test revealed that squirrels spend much more time on a hot plate compared with mice. Although this result could be interpreted as if squirrels are more attracted to hot temperatures than mice, the fact that some of the test plates are noxiously hot (more than 40 °C) strongly argues against such explanation. Furthermore, it appears unlikely that the difference is due to the size of the animals, because rats, which are bigger than ground squirrels, exhibit the same temperature preference as mice (14). In our opinion, a more feasible explanation is that squirrels are more tolerant to hot temperatures than mice. This tolerance could be due to diminished sensitivity at the level of the somatosensory neurons, or due to the suppression of temperature avoidance responses at the level of the central nervous system. Although both scenarios are simultaneously possible, a somatosensory deficit alone would be sufficient to at least partially diminish temperature sensitivity. Indeed, mice with pharmacologically ablated TRPV1-expressing peripheral nociceptors are unable to discriminate between the wide range of temperatures from 25 to 50 °C (13, 26). In the case of squirrels, DRG neurons failed to respond to heating from 22 to 46 °C, but responded to capsaicin, demonstrating that TRPV1 is expressed and functional in these cells. Squirrels avoided eating capsaicin-infused seeds, suggesting that the function of TRPV1 neurons as nociceptors is preserved. Overall, our results strongly suggest that heat tolerance exhibited by the squirrels in the behavioral test is explained, at least partially, by the deficits in heat sensitivity of TRPV1-expressing somatosensory neurons. The neuronal phenotype, in turn, correlates well with the biophysical properties of TRPV1 in two types of heterologous systems, providing a molecular mechanism for heat tolerance in squirrels. We note that the genetic deletion of *Trpv1* in mice leads to the diminution of temperature sensitivity in the highly noxious (more than 50 °C) range (7, 8), suggesting that TRPV1 alone may be insufficient to explain the squirrel temperature phenotype in its entirety.

Decreased thermosensitivity in sqTRPV1 and caTRPV1 did not affect capsaicin and pH sensitivity, demonstrating a modality-specific suppression of TRPV1. We speculate that this decreased thermosensitivity is an evolutionary adaptation targeting a focused aspect of TRPV1 function in the detection of noxious heat through the skin, sparing its role in nonthermal aspects of nociception, inflammation, and thermoregulation (27–31). Arguably, the suppression of heat sensitivity entails the danger of

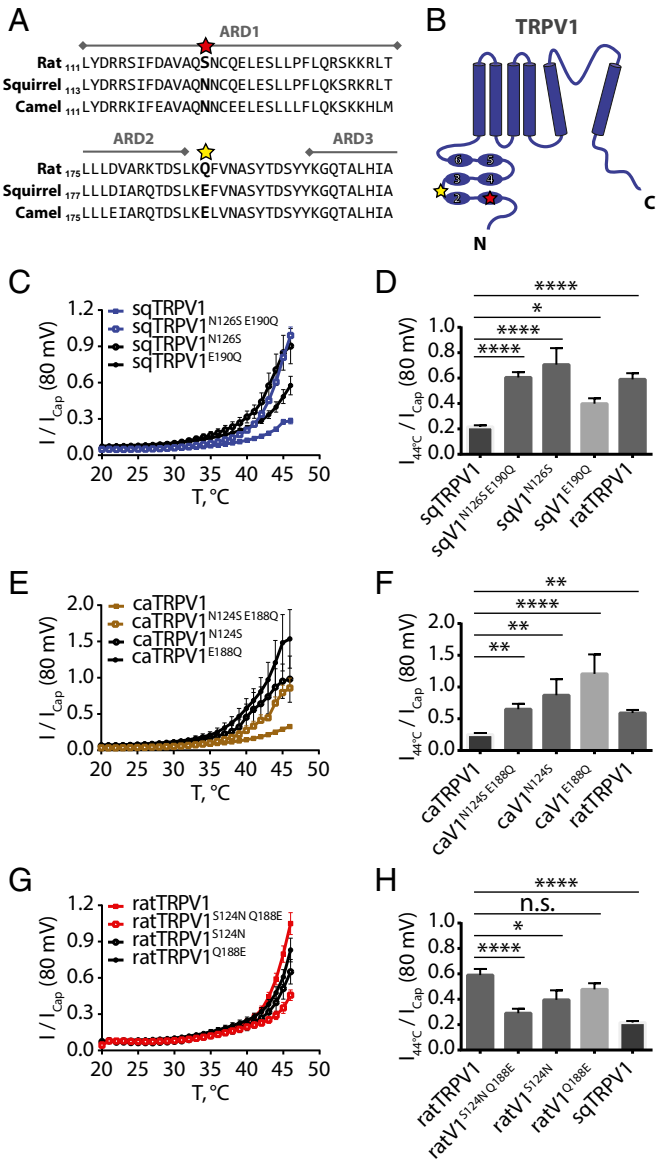

Fig. 5. Single amino acid change modulates TRPV1 heat sensitivity. Amino acid alignment (*A*) and topology diagram (*B*) of TRPV1 channels depicting the locations of the amino acids key to heat sensitivity of rTRPV1, sqTRPV1, and caTRPV1 (yellow and red stars). ARD, ankyrin repeat domain (numbered ovals). (*C*–*G*) Temperature response profiles and quantification of TRPV1 activity at 44 °C for sqTRPV1 (*C* and *D*), caTRPV1 (*E* and *F*), and rTRPV1 (*G* and *H*) mutants obtained by voltage clamp in *Xenopus* oocytes. Currents were recorded in response to voltage ramp from a holding potential of −80 mV. Data are normalized to maximal activity evoked by 5 μM capsaicin. Data shown as mean ± SEM ($n \geq 8$). *$P < 0.05$, **$P < 0.01$, ****$P < 0.0001$, n.s., not significant, one-way ANOVA with Dunnett post hoc test.

accidental burns. However, it may also facilitate the ability of a species to inhabit ecological niches that others find inhospitable.

Although sqTRPV1 and caTRPV1 are poorly heat sensitive, the molecular basis for it is unclear. Our attempts to back-engineer heat sensitivity led to the identification of a pair of amino acids (Asn126/Glu190 and Asn124/Glu188 in squirrel and camel, respectively), which, when mutated to Ser and Gln, respectively, are sufficient to restore temperature gating of the channels to the level of the rat ortholog. Sequence analysis of TRPV1 channels from different species shows that the Asn→Ser and Glu→Gln mutations did not restore a prerequisite heat-sensing sequence of TRPV1, because the Asn/Glu pair is also present in a number of TRPV1 orthologs (cow, vampire bat, coastal mole, chicken, zebrafish), which display robust heat sensitivity in the 28–46 °C range (Table S2) (32, 33). In the crystal structure of the rTRPV1 N-terminal domain, Ser124 is located in the C-terminal part of the inner helix of ankyrin repeat 1, whereas Gln188 is part of the α-helix between the repeats 2 and 3 (Fig. 5 *A* and *B* and Fig. S8) (34). The amino acids are largely solvent exposed and not involved in binding to ATP or other residues. The Asn→Ser and Glu→Gln mutations could, in principle, confer heat sensitivity de novo if they brought a large 2–5 kcal/mol·K change in the molar heat capacity (35, 36). However, even in the case of a double Asn→Ser and Glu→Gln substitution, such change is expected to be too small, on the order of 0.01 kcal/mol·K (37), suggesting a different mechanism.

Our results are in line with the observations that a point mutation in the ankyrin repeat domain can shift temperature responses in TRPV1 of different *Xenopus* species (38) and confer thermal activation to mouse transient receptor potential channel A1 (TRPA1) (39), suggesting a common mechanism of activation. We hypothesize that the mutations affect coupling between the gate and a heat-sensing module(s) located elsewhere in the molecule. The facilitation of heat responses in the presence of capsaicin in sqTRPV1 (Fig. 4 *D* and *E*) suggests that such module could remain functional in the seemingly heat-insensitive channel, whereas the heat-activation curve is shifted beyond the physiologically relevant or experimentally testable temperature due to defects in coupling. Our observations that heat responses in two channels from distantly related species were restored by the same point mutations, and that reciprocal mutations suppress heat sensitivity in rTRPV1 (Fig. 5 *C*–*H*), agree with this hypothesis.

Despite intense research, a heat-sensing module has not been localized for a TRP channel. Studies in TRPV1 showed that heat sensitivity can be altered by mutations in virtually any channel domain (33, 40–46), supporting the idea that molecular determinants of the hypothetical heat-sensing module are not localized in a single topologically defined channel element, but are instead distributed throughout the molecule (35). Although a full-length structure of TRPV1 is currently unavailable, the recent cryo-EM structure of TRPA1 revealed tight interations between the N- and C-termini (47), suggesting that topologically distant domains could be functionally coupled, in which case mutations that affect heat sensing or coupling mechanisms could be functionally indistinguishable. A discrete temperature-sensing module exists in a bacterial voltage-gated sodium channel, where temperature-dependent unfolding of a portion of the C-terminal domain drives channel opening (48). A similar mechanism is conceivable with regard to TRPV1, whereby structural changes in a localized domain lead to channel opening directly or via displacing an inhibitory cofactor. In accordance with a model based on the cryo-EM structure of TRPV1, temperature could act similar to a vanilloid agonist, which opens the channel by displacing phosphatidyinositide from its binding pocket (17). The model unifies agonist and temperature gating of TRPV1 and agrees with our observation that heat sensitivity of sqTRPV1 can be revealed in the presence of capsaicin (Fig. 4 *D* and *E*).

Earlier studies suggested that heat-sensing properties of TRPV1 can be fine-tuned to adapt to physiological needs of warm-blooded species. For example, chicken TRPV1 has a relatively high (46 °C) apparent temperature activation threshold, which can be viewed as an adaptation of the somatosensory system to the high core body temperature of birds (32). In contrast, a TRPV1 isoform from the trigeminal ganglion of vampire bats (apparent activation threshold 30 °C) was suggested to serve as a low radiant heat sensor driving the detection of superficial blood vessels in the bat's warm-blooded prey (33). In both cases,

the scope of the molecular changes that affected heat-sensitive properties of the channel was not clear. Our findings demonstrate that the changes can be minimal, because heat sensitivity of sqTRPV1, caTRPV1, or rTRPV1 can be reversed by as little as a mutation of a single amino acid. Such a low-cost functional plasticity of TRPV1 lends itself as a powerful vehicle to drive evolutionary adaptation, and is apparently exploited by various mammals, including the two species in focus. Indeed, the ecological advantages that squirrels and camels gained owing to their unusual heat resistance could have been achieved through the inexpensive solution of tweaking TRPV1 heat sensitivity via a process of convergent evolution.

Materials and Methods

Animal procedures were performed in compliance with the Institutional Animal Care and Use Committee of Yale University. For the two-plate temperature preference/aversion assay, animals were given a free choice to move on a control (25 °C) or test (25–60 °C) plate, and the time spent on each plate was quantified over 5 min. In the capsaicin ingestion assay, we quantified the number of seeds (infused or not with 1 mM capsaicin) eaten by preconditioned squirrels over 10 min. Cloning, in situ hybridization, ratiometric calcium imaging, and electrophysiology were performed by using standard approaches. See *SI Materials and Methods* for a detailed description.

ACKNOWLEDGMENTS. We thank Jena Goodman, Owen Funk and Jon Matson for technical assistance, and members of the E.O.G. and S.N.B. laboratories for their contributions throughout the project. This study was partly funded by fellowships from the Arnold and Mabel Beckman Foundation and Rita Allen Foundation, NIH Grant 1R01NS091300-01A1 (to E.O.G.), American Heart Association Grant 14SDG17880015, National Science Foundation CAREER Award 1453167 (to S.N.B.), and by the Axle Tech International Endowed Professorship (to D.K.M.). E.R.S. was supported by NIH Training Grant T32HD007094, and W.J.L. was supported by NIH Training Grant T32HG319810.

1. Careau V, Réale D, Garant D, Speakman JR, Humphries MM (2012) Stress-induced rise in body temperature is repeatable in free-ranging Eastern chipmunks (Tamias striatus). *J Comp Physiol B* 182(3):403–414.
2. Chappell MA, Calvo AV, Heller HC (1978) Hypothalamic thermosensitivity and adaptations for heat-storage behavior in three species of chipmunks (Eutamias) from different thermal environments. *J Comp Physiol* 125(2):175–183.
3. Hudson JW, Deavers DR (1973) Metabolism, pulmocutaneous water loss and respiration of eight species of ground squirrels from different environments. *Comp Biochem Physiol A* 45(1):69–100.
4. Jackson HHT (1961) *Mammals of Wisconsin* (Univ Wisconsin Press, Madison).
5. Tulgat R, Schaller GB (1992) Status and distribution of wild Bactrian camels Camelus bactrianus ferus. *Biol Conserv* 62(1):11–19.
6. Caterina MJ, et al. (1997) The capsaicin receptor: A heat-activated ion channel in the pain pathway. *Nature* 389(6653):816–824.
7. Caterina MJ, et al. (2000) Impaired nociception and pain sensation in mice lacking the capsaicin receptor. *Science* 288(5464):306–313.
8. Davis JB, et al. (2000) Vanilloid receptor-1 is essential for inflammatory thermal hyperalgesia. *Nature* 405(6783):183–187.
9. Julius D (2013) TRP channels and pain. *Annu Rev Cell Dev Biol* 29:355–384.
10. Pang Z, et al. (2015) Selective keratinocyte stimulation is sufficient to evoke nociception in mice. *Pain* 156(4):656–665.
11. Bagriantsev SN, Gracheva EO (2015) Molecular mechanisms of temperature adaptation. *J Physiol* 593(16):3483–3491.
12. Gracheva EO, Bagriantsev SN (2015) Evolutionary adaptation to thermosensation. *Curr Opin Neurobiol* 34:67–73.
13. Pogorzala LA, Mishra SK, Hoon MA (2013) The cellular code for mammalian thermosensation. *J Neurosci* 33(13):5533–5541.
14. Balayssac D, et al. (2014) Assessment of thermal sensitivity in rats using the thermal place preference test: Description and application in the study of oxaliplatin-induced acute thermal hypersensitivity and inflammatory pain models. *Behav Pharmacol* 25(2):99–111.
15. Tominaga M, et al. (1998) The cloned capsaicin receptor integrates multiple pain-producing stimuli. *Neuron* 21(3):531–543.
16. Cao E, Liao M, Cheng Y, Julius D (2013) TRPV1 structures in distinct conformations reveal activation mechanisms. *Nature* 504(7478):113–118.
17. Gao Y, Cao E, Julius D, Cheng Y (2016) TRPV1 structures in nanodiscs reveal mechanisms of ligand and lipid action. *Nature* 534(7607):347–351.
18. Cao E, Cordero-Morales JF, Liu B, Qin F, Julius D (2013) TRPV1 channels are intrinsically heat sensitive and negatively regulated by phosphoinositide lipids. *Neuron* 77(4):667–679.
19. Cavanaugh DJ, et al. (2011) Restriction of transient receptor potential vanilloid-1 to the peptidergic subset of primary afferent neurons follows its developmental downregulation in nonpeptidergic neurons. *J Neurosci* 31(28):10119–10127.
20. Kobayashi K, et al. (2005) Distinct expression of TRPM8, TRPA1, and TRPV1 mRNAs in rat primary afferent neurons with adelta/c-fibers and colocalization with trk receptors. *J Comp Neurol* 493(4):596–606.
21. Cavanaugh DJ, et al. (2011) Trpv1 reporter mice reveal highly restricted brain distribution and functional expression in arteriolar smooth muscle cells. *J Neurosci* 31(13):5067–5077.
22. Noël J, et al. (2009) The mechano-activated K+ channels TRAAK and TREK-1 control both warm and cold perception. *EMBO J* 28(9):1308–1318.
23. Schneider ER, Anderson EO, Gracheva EO, Bagriantsev SN (2014) Temperature sensitivity of two-pore (K2P) potassium channels. *Curr Top Membr* 74:113–133.
24. Liu B, Qin F (2016) Use dependence of heat sensitivity of vanilloid receptor TRPV2. *Biophys J* 110(7):1523–1537.
25. Palkar R, Lippoldt EK, McKemy DD (2015) The molecular and cellular basis of thermosensation in mammals. *Curr Opin Neurobiol* 34:14–19.
26. Mishra SK, Tisel SM, Orestes P, Bhangoo SK, Hoon MA (2011) TRPV1-lineage neurons are required for thermal sensation. *EMBO J* 30(3):582–593.
27. Garami A, et al. (2011) Thermoregulatory phenotype of the Trpv1 knockout mouse: Thermoeffector dysbalance with hyperkinesis. *J Neurosci* 31(5):1721–1733.
28. Feketa VV, Balasubramanian A, Flores CM, Player MR, Marrelli SP (2013) Shivering and tachycardic responses to external cooling in mice are substantially suppressed by TRPV1 activation but not by TRPM8 inhibition. *Am J Physiol Regul Integr Comp Physiol* 305(9):R1040–R1050.
29. Jordt SE, Tominaga M, Julius D (2000) Acid potentiation of the capsaicin receptor determined by a key extracellular site. *Proc Natl Acad Sci USA* 97(14):8134–8139.
30. Chuang HH, et al. (2001) Bradykinin and nerve growth factor release the capsaicin receptor from PtdIns(4,5)P2-mediated inhibition. *Nature* 411(6840):957–962.
31. Hanack C, et al. (2015) GABA blocks pathological but not acute TRPV1 pain signals. *Cell* 160(4):759–770.
32. Jordt SE, Julius D (2002) Molecular basis for species-specific sensitivity to "hot" chili peppers. *Cell* 108(3):421–430.
33. Gracheva EO, et al. (2011) Ganglion-specific splicing of TRPV1 underlies infrared sensation in vampire bats. *Nature* 476(7358):88–91.
34. Lishko PV, Procko E, Jin X, Phelps CB, Gaudet R (2007) The ankyrin repeats of TRPV1 bind multiple ligands and modulate channel sensitivity. *Neuron* 54(6):905–918.
35. Clapham DE, Miller C (2011) A thermodynamic framework for understanding temperature sensing by transient receptor potential (TRP) channels. *Proc Natl Acad Sci USA* 108(49):19492–19497.
36. Chowdhury S, Jarecki BW, Chanda B (2014) A molecular framework for temperature-dependent gating of ion channels. *Cell* 158(5):1148–1158.
37. Makhatadze GI (1998) Heat capacities of amino acids, peptides and proteins. *Biophys Chem* 71(2-3):133–156.
38. Saito S, et al. (2016) Evolution of heat sensors drove shifts in thermosensation between Xenopus species adapted to different thermal niches. *J Biol Chem* 291(21):11446–11459.
39. Jabba S, et al. (2014) Directionality of temperature activation in mouse TRPA1 ion channel can be inverted by single-point mutations in ankyrin repeat six. *Neuron* 82(5):1017–1031.
40. Brauchi S, Orta G, Salazar M, Rosenmann E, Latorre R (2006) A hot-sensing cold receptor: C-terminal domain determines thermosensation in transient receptor potential channels. *J Neurosci* 26(18):4835–4840.
41. Grandl J, et al. (2010) Temperature-induced opening of TRPV1 ion channel is stabilized by the pore domain. *Nat Neurosci* 13(6):708–714.
42. Prescott ED, Julius D (2003) A modular PIP2 binding site as a determinant of capsaicin receptor sensitivity. *Science* 300(5623):1284–1288.
43. Yang F, Cui Y, Wang K, Zheng J (2010) Thermosensitive TRP channel pore turret is part of the temperature activation pathway. *Proc Natl Acad Sci USA* 107(15):7083–7088.
44. Yao J, Liu B, Qin F (2011) Modular thermal sensors in temperature-gated transient receptor potential (TRP) channels. *Proc Natl Acad Sci USA* 108(27):11109–11114.
45. Bae C, et al. (2016) Structural insights into the mechanism of activation of the TRPV1 channel by a membrane-bound tarantula toxin. *eLife* 5:e11273.
46. Jara-Oseguera A, Bae C, Swartz KJ (2016) An external sodium ion binding site controls allosteric gating in TRPV1 channels. *eLife* 5:e13356.
47. Paulsen CE, Armache JP, Gao Y, Cheng Y, Julius D (2015) Structure of the TRPA1 ion channel suggests regulatory mechanisms. *Nature* 520(7548):511–517.
48. Arrigoni C, et al. (2016) Unfolding of a temperature-sensitive domain controls voltage-gated channel activation. *Cell* 164(5):922–936.
49. Bagriantsev SN, Peyronnet R, Clark KA, Honoré E, Minor DL, Jr (2011) Multiple modalities converge on a common gate to control K2P channel function. *EMBO J* 30(17):3594–3606.

Supporting Information

Laursen et al. 10.1073/pnas.1604269113

SI Materials and Methods

Animals. Animals were housed in a pathogen-free facility at Yale University. All animal procedures were performed in compliance with the Institutional Animal Care and Use Committee of Yale University. Thirteen-lined ground squirrels were maintained on a diet of dog food (Iams) supplemented with sunflower seeds, superworms, and fresh vegetables. Trpv1$^{-/-}$ mice were a gift from Sven-Eric Jordt (Duke University, Durham, NC). Mice and squirrels were housed on a 12-h light/dark cycle under standard laboratory conditions with ad libitum access to food and water.

Temperature Preference and Capsaicin Ingestion Assays. Behavioral experiments on mice and active squirrels were performed in May–July. For the two-plate temperature preference/aversion assay, animals were placed into a chamber containing one floor plate set to a control temperature of 25 °C and the other set to a test temperature between 25 and 60 °C (T2CT). Animals were recorded as they freely explored both sides of the chamber for a total of 5 min. There was a minimum of 1 d between test days. Plate order was reversed between groups and test days.

The capsaicin ingestion assay consisted of two experimental days. Initially, animals were randomly presented with either 10 vehicle-treated sunflower seeds or seeds treated with either the oil from habanero peppers or a solution of 1 mM capsaicin. The number of seeds eaten in a 10-min time interval was quantified. After 48 h, animals were presented with 10 sunflower seeds of the other treatment group (vehicle or pepper). Behavioral responses were monitored by video recording. With the exception of the additional seeds presented during testing, animals were maintained on their standard diet throughout the course of the experiment.

Calcium Imaging. Animals were euthanized via CO_2 inhalation followed by decapitation. Dorsal root ganglia were dissected into ice-cold PBS then briefly treated with collagenase P (1 mg/mL in HBSS, 15 min, 37 °C) followed by 0.25% trypsin (10 min, 37 °C). Finally, tissue was suspended in DMEM Complete media supplemented with 10% (vol/vol) FBS and penicillin/streptomycin and mechanically dissociated by using a plastic-tipped pipette before being plated on BD Matrigel-coated coverslips and incubated at 37 °C. After neurons were adherent (~2 h), coverslips were loaded with 10 μM Fura 2-AM (Invitrogen) and 0.02% Pluronic F-127 for 1 h at room temperature. Images were obtained by using Axio-Observer.Z1 inverted microscope (Zeiss) equipped with an Orca-Flash4.0 camera (Hamamatsu) using the MetaFluor software (Molecular Devices). For loading and imaging, cells were maintained in physiological Ringer's solution (pH 7.4) containing (in mM): 140 NaCl, 5 KCl, 10 Hepes, 2 $CaCl_2$, 2 $MgCl_2$, and 10 D-glucose. Capsaicin (Sigma-Aldrich) was freshly diluted from 100 mM stock dissolved in DMSO. Heat ramps were applied by using the SC-20 in-line heater-cooler and CL-200A Bipolar Temperature controller (Warner), with bath temperature monitored via a thermistor situated in the imaging chamber. At the end of imaging, neurons were identified based on their responses to high K^+ Ringer's solution containing (in mM): 10 NaCl, 135 KCl, 10 Hepes, 2 $CaCl_2$, 2 $MgCl_2$, and 10 D-glucose.

Cloning, Gene Synthesis, Mutagenesis, and Plasmids. Rat *Trpv1* in pMO vector was generously provided by David Julius (University of California, San Francisco). Mouse *Kcnk2* (TREK1/K_{2P}2.1, NP_034737.2) cloned into pGEMHE was described (49). Squirrel *Trpv1* (KU877439) was cloned from cDNA from dorsal root ganglia by using the following primers: forward 5′-ATGAAGAAGTGGGCTAACTTAGAC-3′; reverse 5′-GGTCACACTGCTGACAGG-3′. Squirrel *Kcnk2* (TREK1/K_{2P}2.1, protein sequence identical to XP_005335026.1) was cloned by using forward 5′-ATGCTTCCCAGCGCCTCG–3′; reverse 5′- CTATTTAATGTTCTCAATAACAGCAATCTCTTCA-3′ primers. Mouse *Trpv1* (NP_001001445) was cloned from cDNA from dorsal root ganglia by using the following primers: forward 5′-GCAAATTGGGCCACAGAAGATC-3′; reverse 5′-GCAGAGTACAGCCAGCCAAC -3′. Camel *Trpv1* was synthesized by Genewiz based on the predicted sequence from the wild Bactrian camel (*Camelus ferus*) genome (XM_006172536.1). The camel *Trpv1* sequence is obtained by automated computational analysis of the full *C. ferus* genome (NW_006210217.1). Annotation was done by using the gene prediction method Gnomon and supported by mRNA evidence including transcriptomes assembled from RNA extracted from 10 tissue types from Bactrian and dromedary camels (*Camelus bactrianus* and *Camelus dromedarius*). Squirrel, mouse and camel *Trpv1* orthologs were subcloned into the pMO vector. Point mutations and chimeras were generated by using the QuikChange Site-Directed mutagenesis kit (Agilent) and overlapping PCR. All constructs were verified by full-length sequencing.

RNA in Situ Hybridization. Dorsal root ganglia were dissected and fixed overnight in 4% (vol/vol) paraformaldehyde in PBS. RNA in situ hybridization was performed on cryostat sections (12 μm) by using digoxigenin-labeled cRNA probes generated by T7/T3 in vitro transcription reaction using a full-length *Trpv1* cDNA. Signal was developed with alkaline phosphatase-conjugated anti-digoxigenin Fab fragments according to the manufacturer's instructions (Roche).

Oocyte Electrophysiology. Oocytes were surgically extracted from *Xenopus laevis* in accordance with procedures approved by the Institutional Animal Care and Use Committee of Yale University. Oocytes were cultured at 18 °C in ND96 media containing (mM): 2 KCl, 96 NaCl, 2.0 $MgCl_2$, 1.8 $CaCl_2$, 5 Hepes/NaOH pH 7.4 and supplemented with penicillin/streptomycin. cRNA was synthesized by in vitro transcription from linearized plasmids using the mMessage mMachine kit (Ambion), and 10–20 ng of RNA was injected per oocyte. Electrophysiological recording were performed by two-electrode voltage clamp 1–6 d after injection using the OC-725 amplifier. Whole-cell currents were elicited by 2-s voltage ramp from −150 to +90 mV from a holding potential of −80 mV in ND96 pH 7.4 (NaOH), filtered at 1 kHz, sampled at 5 kHz using the Digidata 1440 digitizer and recorded in pCLAMP 10.3 software (Molecular Devices). Oocytes that displayed currents in excess of 20 μA at 80 mV were discarded from analysis. Heat ramps were applied by using the SC-20 in-line heater/cooler and CL-100 Temperature controller (Warner), with bath temperature monitored via a thermistor situated adjacent to the oocyte. The peak-to-peak time interval between first and second heat applications (with or without 100 nM capsaicin) was 4 min, and the interval between second heat application and final 5 μM capsaicin application was 4.5 min. For TRPV1 pH activation experiments, ND96 without Ca^{2+} supplemented with 0.1 mM $BaCl_2$ was used. Solutions were buffered to pH 7.4 and 6.8 with 5 mM Hepes, to pH 6.3, 6.0, and 5.5 with 10 mM Mes, to pH 5.0, 4.5, and 3.5 with 10 mM citric acid; pH was adjusted with NaOH. To obtain dose–response curves for capsaicin and protons, whole-cell currents were measured at +80 mV were fitted to a modified Hill equation: $I = I_{min} + (I_{max} - I_{min})/(1 + ([C]_{1/2}/[C])^H)$, where I_{min} and I_{max} are the minimal and maximal current values, respectively,

$[C]_{1/2}$ is the half-maximal effective concentration of capsaicin or protons, and H is the Hill coefficient. To obtain temperature–response curves for TREK1, whole-cell currents measured at +40 mV were fitted to a modified Boltzmann equation: $I = I_{min} + (I_{max} - I_{min})/(1 + \exp^{(T_{1/2}-T)/S})$, where $T_{1/2}$ is the half-maximal effective temperature, and S is the slope.

HEK293 Electrophysiology. Electrophysiological recordings in HEK293 cells transfected with rTRPV1 and sqTRPV1 were made by using an Axon 200B amplifier, digitized using a Digidata 1440 and recorded in pCLAMP 10.3 software (Molecular Devices). Currents were evoked in the whole-cell configuration by a 1-s voltage ramp from −100 to +60 mV, from a −60 mV holding potential, filtered at 2 kHz and sampled at 5 kHz. Recording solutions (Bath, in mM: 140 NCl, 5 KCl, 2 $MgCl_2$, 2 $CaCl_2$, 10 D-glucose, 10 Hepes/NaOH pH 7.4. Pipette, in mM: 150 KCl, 3 $MgCl_2$, 5 EDTA, 10 Hepes/KOH pH 7.2). Heat ramps were applied by heating the perfusing solution using the SC-20 in-line heater-cooler and CL-200A Bipolar Temperature controller (Warner). Bath temperature was measured by a thermistor situated in the recording chamber.

Statistical Analysis. Data were obtained from at least two independent experiments and analyzed with GraphPad Prism 6.0 (GraphPad Software) and probed for significance by using the statistical test described in the figure legends.

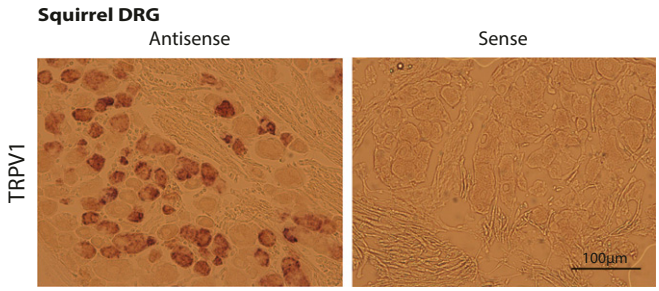

Fig. S1. *Trpv1* is expressed in squirrel dorsal root ganglia. Exemplar RNA in situ hybridization images of squirrel dorsal root ganglia show *Trpv1* expression in somatosensory neurons.

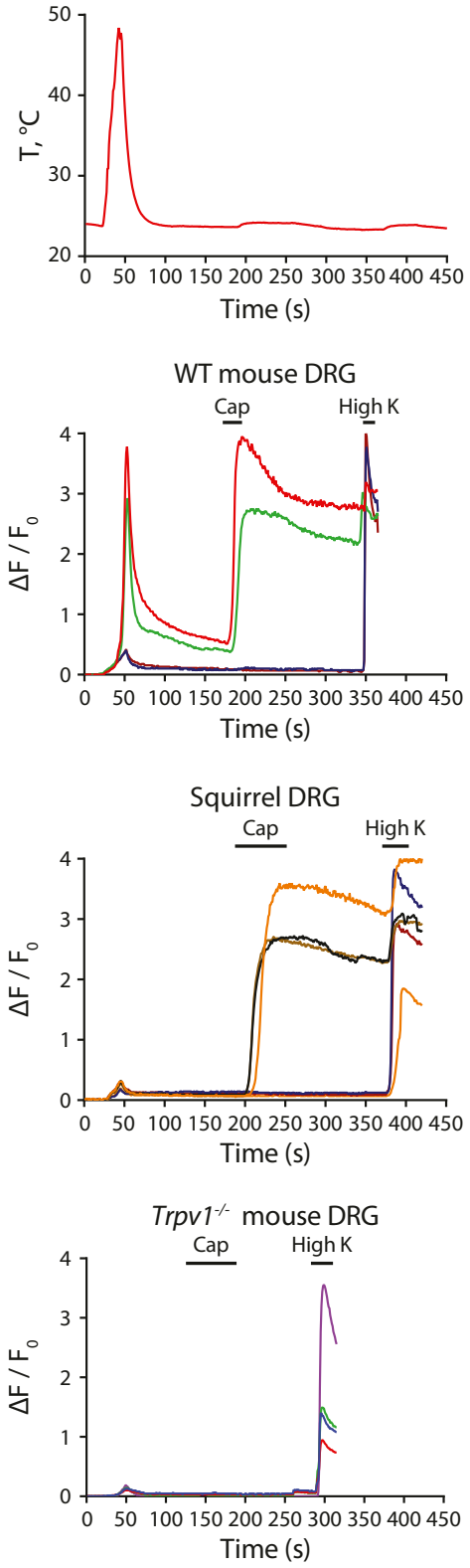

Fig. S2. Temperature sensitivity of dissociated neurons from dorsal root ganglia. Shown are baseline-normalized changes in intracellular Ca^{2+} recorded from the neurons in the zoomed insets of Fig. 1*C* by ratiometric calcium imaging at different temperatures. Neurons were stimulated by heat ramp as shown on *Top*, followed by application of 1 μM capsaicin and 135 mM KCl solution as indicated by horizontal bars.

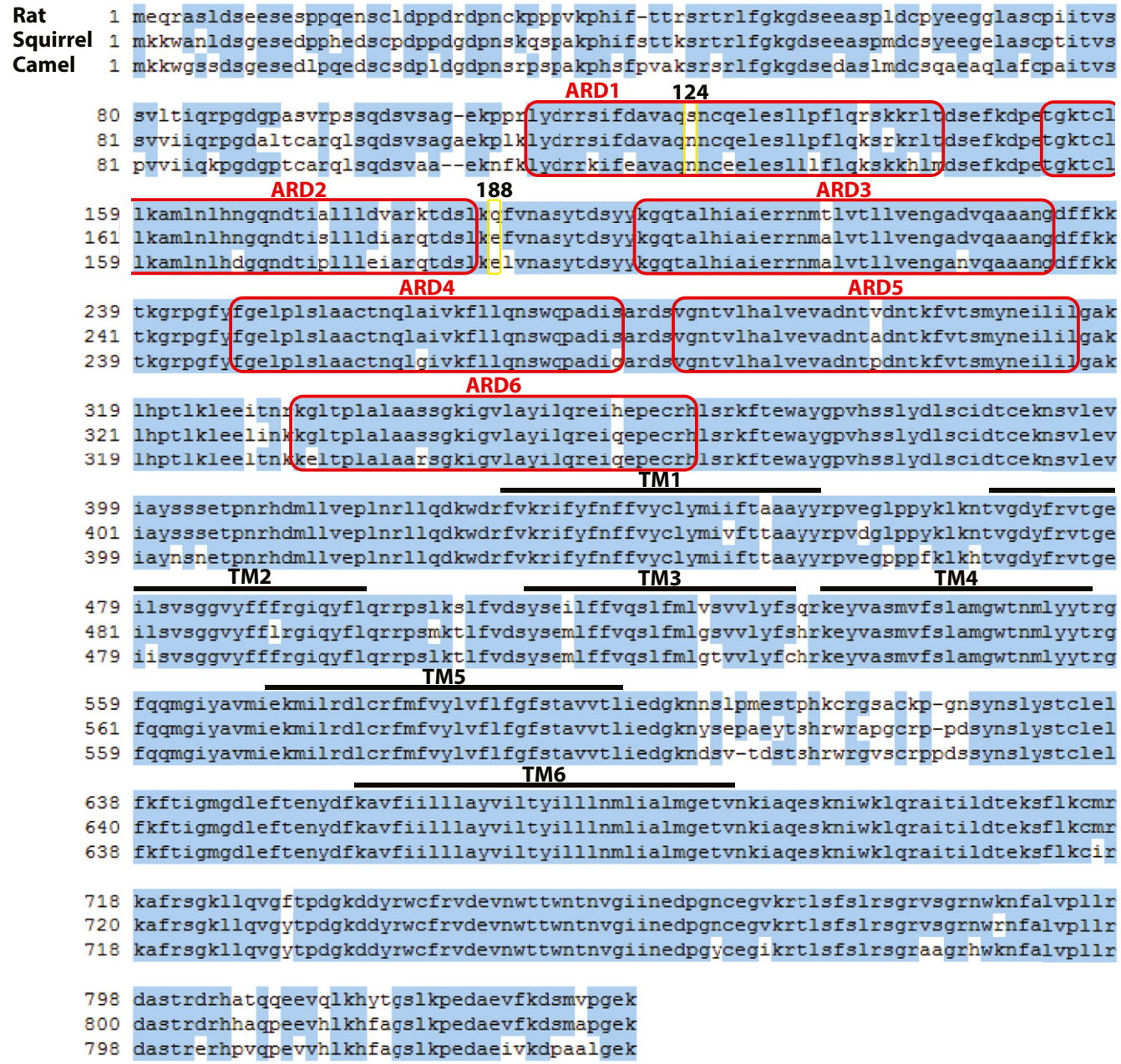

Fig. S3. Alignment of amino acid sequences of rTRPV1 and sqTRPV1. Amino acid alignment of rTRPV1 (NP_114188), sqTRPV1 (KU877439), and caTRPV1 (XP_006172598) orthologs. SqTRPV1 and caTRPV1 are 89% identical to each other, and 90% and 85% identical to rTRPV1, respectively. The locations of ankyrin repeats (red boxes) and transmembrane domains (black bars) are depicted, along with the two amino acids identified in this study as being involved in temperature sensitivity (yellow boxes).

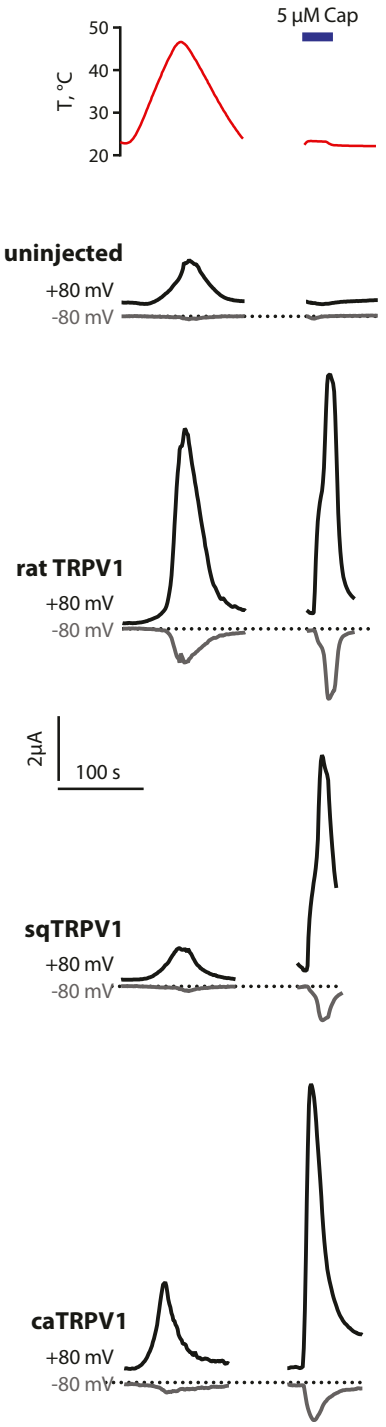

Fig. S4. Voltage-clamp recordings of temperature and chemical responses of TRPV1 orthologs. Exemplar traces showing temperature- and capsaicin-evoked activity from control (uninjected) or TRPV1-expressing *Xenopus* oocytes measured at +80 mV and −80 mV by two-electrode voltage clamp. Oocytes were stimulated by a heat ramp followed by 5 µM capsaicin as indicated in *Top*.

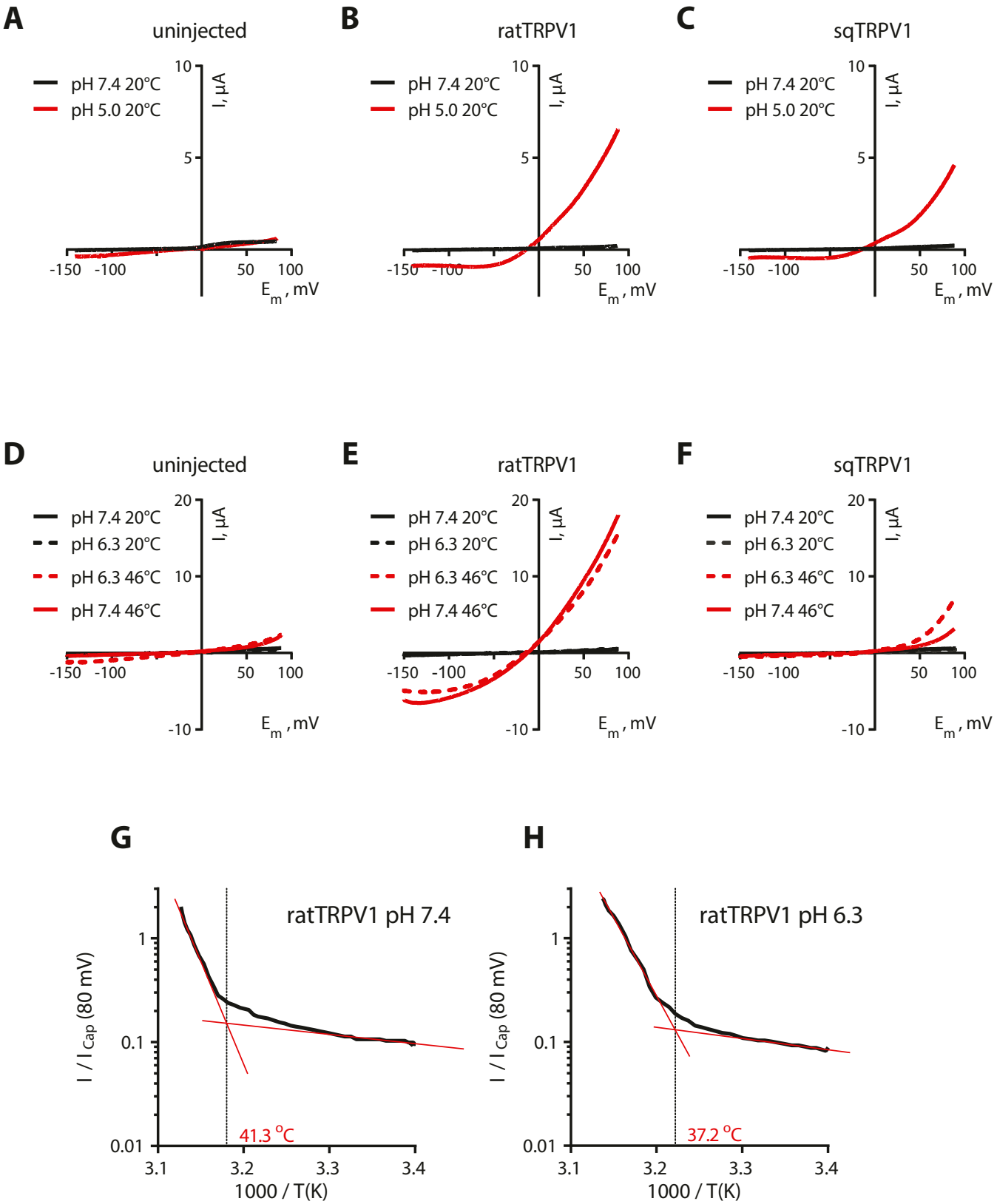

Fig. S5. Sensitivity of TRPV1 to acidic pH. (*A*–*C*) Exemplar current–voltage plots of responses to low pH (pH 5.0) obtained by two-electrode voltage clamp in uninjected *Xenopus* oocytes (*A*) and those expressing rTRPV1 (*B*) or sqTRPV1 (*C*). (*D*–*F*) Exemplar current–voltage plots of responses to pH 6.3 at both room temperature and 46 °C in uninjected *Xenopus* oocytes (*D*) and those expressing rTRPV1 (*E*) or sqTRPV1 (*F*). (*G* and *H*) Arrhenius plots show difference in thermal threshold for rTRPV1 heated in pH 7.4 (*G*) compared with pH 6.3 (*H*). Currents were recorded during voltage ramp from a holding potential of −80 mV and normalized to maximum response to 5 µM capsaicin ($n \geq 6$).

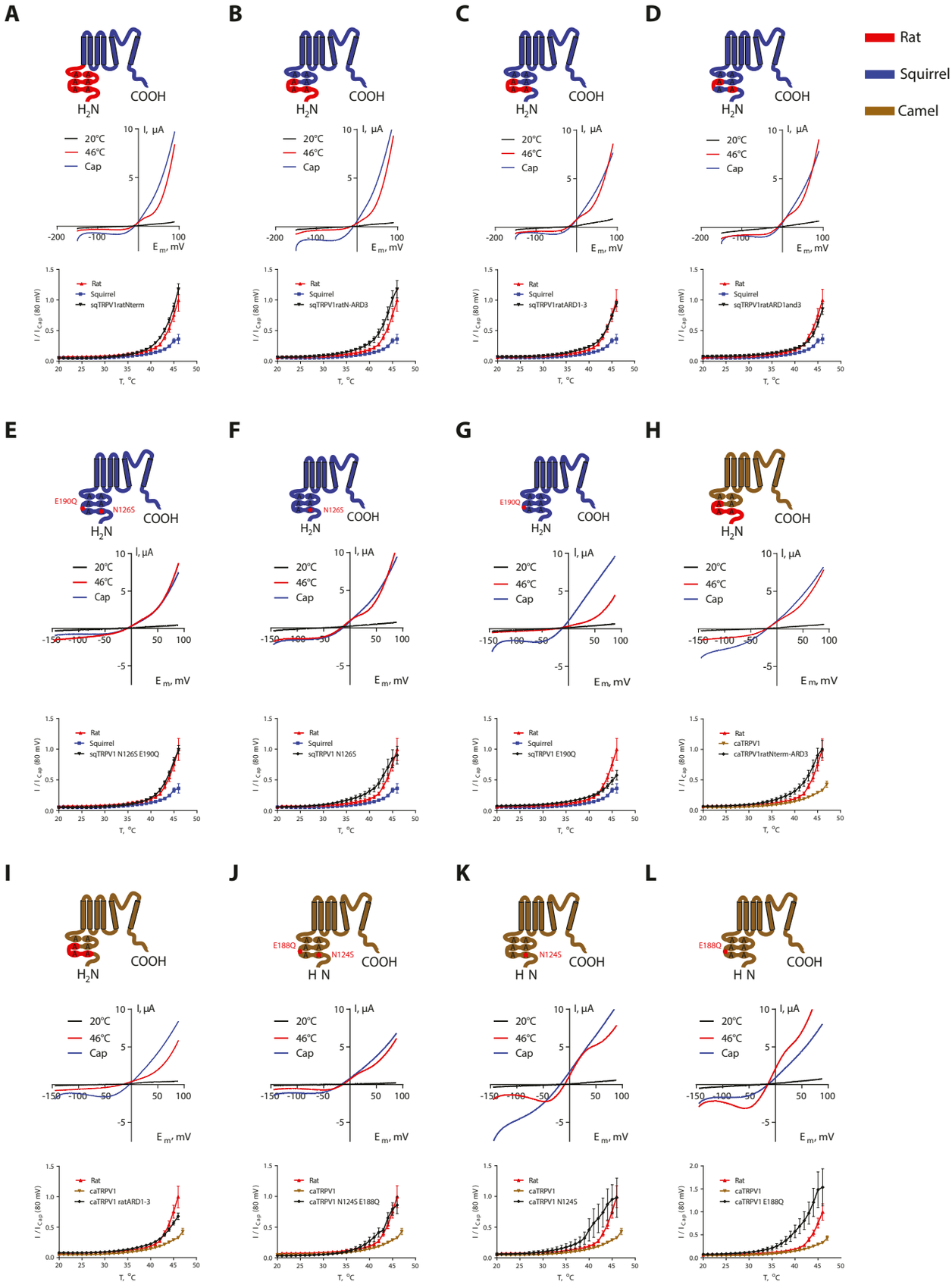

Fig. S6. Temperature sensitivity of chimeric TRPV1 channels. (*A*–*L*) Shown are topology diagrams (*Top*), exemplar current–voltage plots (*Middle*), and quantification of temperature responses (*Bottom*) of TRPV1 chimeras recorded by two-electrode voltage clamp in *Xenopus* oocytes. Currents were elicited by a voltage ramp from a holding potential of −80 mV. Data shown as mean ± SEM from 8 to 31 oocytes.

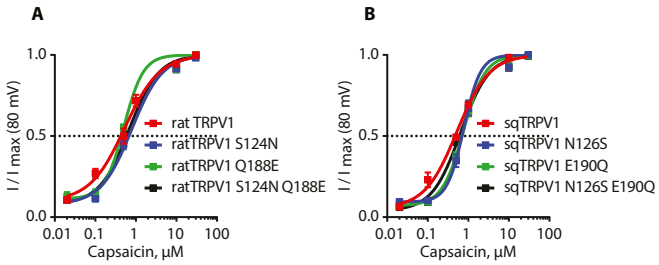

Fig. S7. Capsaicin sensitivity of mutant TRPV1 channels. Capsaicin dose–response curves for mutant rTRPV1 (*A*) and sqTRPV1 (*B*) channels recorded by two-electrode clamp in *Xenopus* oocytes. Currents were elicited by a voltage ramp from a holding potential of −80 mV. (n = 8–14).

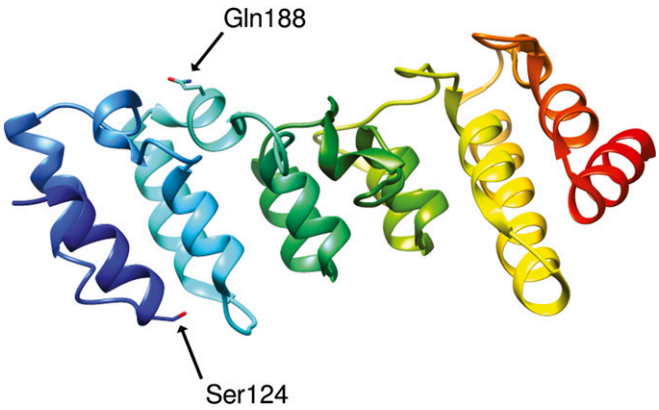

Fig. S8. Structure of the ankyrin repeat domain of TRPV1. The crystal structure of the ankyrin repeat domain of rat TRPV1 (PDB ID code: 2PNN) is shown along with the locations of the specific amino acids relevant to this study.

Table S1. Capsaicin sensitivity of TRPV1 orthologs and mutants expressed in *Xenopus* oocytes

Channel	EC_{50} mean ± SEM, nM	*n*
rTRPV1	527.1 ± 53	21
sqTRPV1	528.5 ± 32	10
caTRPV1	609.6 ± 36	10
mTRPV1	775.6 ± 52	12
$rTRPV1^{S124N}$	785.0 ± 67	14
$rTRPV1^{Q188E}$	506.8 ± 31	11
$rTRPV1^{S124N/Q188E}$	679.1 ± 68	11
$sqTRPV1^{N126S}$	772.5 ± 38	8
$sqTRPV1^{E190Q}$	766.7 ± 32	9
$sqTRPV1^{N126S/E190Q}$	643.9 ± 28	9

Table S2. Conservation of the rat Ser124 and Gln188 sites among heat-activated and heat-resistant TRPV1 orthologs

TRPV1 (GenBank accession no.)	Site 1 (rat Ser124)	Site 2 (rat Gln188)	Apparent T_{act} threshold in heterologous cells, °C	Overall identity with rat TRPV1, %	Source
Rat (NM_031982) *Rattus norvegicus*	Ser124	Gln188	42	—	6, 15
Squirrel (KU877439) *Ictidomys tridecemlineatus*	Asn126	Glu190	No activation up to 46	85	This study
Camel (XM_006172536) *Camelus ferus*	Asn124	Glu188	No activation up to 46	85	This study
Camel (XM_010950234) *Camelus bactrianus*	Asn124	Glu188	N/A	84	—
Camel (XM_010987938) *Camelus dromedarius*	Asn124	Glu188	N/A	85	—
Cow (DAA18892) *Bos taurus*	Asn123	Glu187	40.5	85	33
Vampire Bat (JN006855, JN006856) *Desmondus rotundus*	Asn125	Glu189	31, 40	85	33
Coastal Mole (JN006861, JN006862) *Scapanus orarius*	Asn126	Glu190	31, 38	86	33
Chicken (NM_204572) *Gallus gallus*	Gly131	Glu195	46	66	32
Zebrafish (XP_005165384) *Danio rerio*	Gly92	Asn154	33	44	33